The High Temperature Oxidation of Al-4.2 Wt Pct Mg Alloy

D. J. FIELD, G. M. SCAMANS, and E. P. BUTLER

The high temperature oxidation of Al-Mg alloys is characterized by the rapid formation of thick, micro-crystalline oxide films. The oxidation kinetics of an Al-4.2 wt pct Mg alloy under dry and moist 20 pct O_2/Ar have been measured, and oxide films grown on bulk specimens complementary to the weight gain curves have been characterized using electron optical techniques (TEM, SEM). Initial oxidation takes place by the nucleation and growth of primary crystalline oxides at the oxide/metal interface and by the formation of secondary oxides of MgO by the reduction of the original amorphous over-layer of γ-Al_2O_3 by Mg. Subsequent oxidation is dominated by the further nucleation and growth of primary oxides. The presence of water vapor in the oxidizing environment initially reduces oxidation rates through a modification of the mechanical properties of the amorphous overlayer but does not affect the overall oxidation mechanism. A microstructural model has been developed which describes oxidation of Al-Mg alloys in terms of fracture of the original air-formed film by primary MgO nucleation and growth and modification to this film by the presence of water vapor in the oxidizing environment.

I. INTRODUCTION

MAGNESIUM additions to aluminum form a technologically important alloy system having good mechanical and physical properties in conjunction with excellent aqueous corrosion resistance. However, these alloys oxidize rapidly both when molten and during high temperature heat treatment of solid product forms, giving rise to thick surface films of magnesium oxide which may be accompanied by severe metal blistering in moist environments. Before further processing can take place, the surface films must be removed which results in an expensive loss of metal, and can make processes such as scrap recycling commercially uneconomical. Methods of controlling the rapid oxidation of Al-Mg alloys have been established, such as by trace-alloying additions, with the most effective additive being toxic Be.[1]

The oxidation kinetics of Al-Mg alloys have been measured thermogravimetrically by several investigators[2,3,4] but when comparing weight gains the surface preparation of specimens prior to oxidation appears to be an important factor, affecting overall weight gains by orders of magnitude, and this factor has not always been closely controlled. From the literature evidence it is clear that weight gain measurements alone have shed relatively little light on the oxidation mechanism(s) operating during the high temperature oxidation of Al-Mg alloys. In recent years the application of modern TEM techniques to high temperature oxidation[5] has become more commonplace, and microstructural studies in conjunction with thermogravimetry offer the opportunity of gathering structural information which can then be related to the oxidation weight gain. This approach was adopted in this investigation.

D. J. FIELD, Research Scientist, and G. M. SCAMANS, Principal Scientist, are with Alcan International Limited, Banbury Laboratories, Banbury, Oxon OX16 7SP, England. E. P. BUTLER, formerly at Imperial College, London, is Principal Scientist with Alcan International Limited, Banbury.

Manuscript submitted August 8, 1985.

Aluminum and Aluminum Alloy Oxidation

During the initial stages of oxidation over a wide range of conditions, aluminum and aluminum alloys rapidly develop a thin tenacious film of amorphous γ-Al_2O_3.[5] This oxide layer provides a barrier between the metal substrate and the environment, and it is this film which has been shown to control the early stages of crystalline oxide formation at high temperatures.[6–9] At temperatures above about 425 to 450 °C, the amorphous γ-Al_2O_3 overlayer undergoes a discontinuous change in structure.[6] Rapid migration of oxygen to the oxide/metal interface is readily detectable at these temperatures and is evidenced by the nucleation and growth above about 450 °C of crystalline γ-Al_2O_3 as a new phase below the amorphous layer. Growth of amorphous γ-Al_2O_3 continues by cation diffusion to the oxide-oxygen interface in a fashion of mutual independence with respect to any underlying crystallites of γ-Al_2O_3 which form at the oxide/metal interface and penetrate down into the metal after a temperature-dependent induction period.[5,6,7] The high temperature surface films which develop on aluminum alloys are characteristically duplex, consisting of both crystalline and amorphous oxides.[8] The amorphous film is important in the initial stage of oxidation as the film thickness and/or ion transport properties change with alloy addition.[7,9] In Al-Cu alloys,[9] for example, the dielectric constant of the crystalline γ-Al_2O_3 which develops is much lower than that of the crystalline γ-Al_2O_3 formed on pure aluminum, a result explained in terms of the reduction of cation vacancies due to doping of the γ-Al_2O_3 by copper ions.

The oxidation of Al-Mg alloys has been the subject of many studies: by thermogravimetry,[2,3,4] X-ray diffractometry of oxide powders[2] and electron microscopy of stripped[1,10] or back-polished films, and by *ex situ* oxidation of evaporated films[13] or *in situ* oxidation of thin foil samples.[7,8] Smeltzer[2] measured the oxidation weight gains and vacuum evaporation losses of an Al-3 wt pct Mg alloy. Oxidation was found to be rapid at temperatures above 400 °C and in the temperature range 350 to 550 °C, the kinetics were found to characteristically decrease with time, subsequently giving way to approximately linear kinetics at weight gains greater than 10 $\mu g/cm^2$. Oxide powder scraped from Al-3 wt pct Mg oxidized for 60 hours at

550 °C in dry oxygen consisted of Al, MgO, and $MgAl_2O_4$. Examination of stripped films on Al-3 wt pct Mg by Brock and Heine[10] showed that crystalline oxides of MgO with a platelet morphology approximately 2000 Å in diameter were present located at the oxide/metal interface. Grauer and Schmoker[11] (using data given previously by Ritchie *et al.*[13]) constructed an Al-Mg-O_2 stability diagram and defined magnesium-alloy compositions over which various crystalline oxides would be stable. Oxidation of three aluminum alloys containing 0.17, 1.55, and 4.6 wt pct Mg was conducted in dry oxygen. The two most concentrated alloys exhibited three branches of the oxidation weight gain curves typified by:

(i) an initial logarithmic rise due to thickening of the original overlying amorphous film of γ-Al_2O_3,
(ii) an adjacent, S-shaped branch as a result of crystalline film formation at the oxide metal interface, and
(iii) a final linear increase in weight due to further nucleation and growth of crystalline oxides.

The oxidation products were crystalline MgO together with amorphous γ-Al_2O_3. With time, the 1.55 wt pct Mg alloy exhibited two stages of crystalline MgO nucleation and growth. Initially fine MgO developed within the amorphous overlayer of γ-Al_2O_3, and with further oxidation complete coverage by MgO crystallites of the oxide/metal interface was observed. The appearance of these crystals was correlated with the transition from parabolic type to linear kinetics on this alloy. Low oxygen partial pressures ($\sim 10^{-4}$ torr) promoted $MgAl_2O_4$ formation at 475 °C in a manner similar to the growth of crystalline γ-Al_2O_3 on pure aluminum.

The important effect of furnace atmosphere on Al-Mg oxidation was investigated by Hine and Guminski[12] for a number of compositions. Under dry oxidizing conditions the weight gains were shown to increase as a function of magnesium level. In the temperature range 480 °C to 520 °C, the presence of 0.5 to 1.5 v/v of H_2O in the oxidizing environment gave rise to lower overall weight gains as compared with dry conditions over periods of oxidation from 25 to 100 hours. However, from about 100 hours the reaction rates were found to increase progressively; this rise was attributed to the increase in specific surface area of the specimens due to hydrogen induced alloy blistering and blister rupture. In contrast, Cochran and Sleppy,[3] who investigated the oxidation of an Al-2.35 pct Mg alloy under dry and wet conditions over a broadly similar temperature range, found that water vapor additions to the oxidizing environment enhanced the overall oxidation weight gains at all times. The authors also attributed this increase in the weight gain curves to an increase in specific specimen area due to hydrogen blistering.

In situ observations[8] on Al-5 wt pct Mg have indicated that oxygen transport is enhanced by magnesium doping of the amorphous γ-Al_2O_3 film giving rise to the rapid nucleation and growth of crystalline magnesium oxides at the oxide/metal interface by direct oxidation. The nucleation and growth of these crystalline oxides is analogous to the formation of crystalline γ-Al_2O_3 on pure aluminum above 475 °C. Diffraction evidence showed diffuse rings analyzed as MgO in addition to the spinel reflections. Hence the crystalline magnesium oxide films are duplex with MgO developing either by direct oxidation at the oxide/metal interface or by secondary reduction of the amorphous overlying film,[8,13] according to:

$$3Mg + \gamma\text{-}Al_2O_3 \rightarrow 3MgO + 2Al$$
$$\Delta G^\circ_{800\,K} = -90\ \text{kJ mol}^{-1}O_2 \qquad [1]$$

The oxides resulting from these two independent oxidation mechanisms have been termed primary and secondary, respectively.[8]

II. EXPERIMENTAL

The Al-Mg alloy used in this study was prepared from super-purity components and produced as a small chill cast ingot. Chemical analysis showed the alloy composition in weight pct to be Al-4.2Mg, ≤0.01Fe, ≤0.01Si, ≤0.01Zn, ≤0.01Cr, ≤0.01Pb, 0.012Ti, ≤0.001Mn, 0.004Cu. Following hot rolling the material was cold rolled to 0.2 mm section. Prior to the final cold reduction, the alloy sheet was etched in 2 N NaOH solution at 70 °C for 90 seconds to remove the surface layers depleted in magnesium and then desmutted in 2 N nitric acid.

Rectangular specimen coupons (1.5 × 2.0 cm) for both thermogravimetry and electron microscopy were cut and annealed under a high purity argon atmosphere for 10 minutes at 450 °C. Before oxidation all specimens were given a standard surface treatment of electropolishing in a 20 pct perchloric acid/80 pct ethanol electrolyte at −20 °C and 30 V potential, followed by several rinses in fresh anhydrous methanol and subsequent storage for 14 days in a desiccator at 0 pct R.H. in order to enable a reproducible air-formed film of amorphous γ-Al_2O_3 to develop.[14] All reagents used in surface preparation were of Analar grade and were discarded after use. Oxidation weight gains were measured using a continuously recording thermogravimetric balance with a resolution of ±2.5 μg, utilizing a dynamic atmosphere with a flow rate of 100 cm^3/minute to overcome buoyancy effects. The oxidation temperature was monitored by a thermocouple placed close to the specimen, and the thermal response of the system was such that within 5 minutes of initiating a run, the specimen was within 5 °C of the desired temperature. The oxidizing atmosphere employed was a synthetic air mixture of high purity 20 pct oxygen/80 pct argon and admitted to the thermobalance either dried (4 ppm H_2O) or water vapor saturated at 20 °C (17.5 torr H_2O).

Oxide films were studied by electron microscopy at points corresponding to significant positions along the oxidation weight gain curves. Films compatible with examination by 100 kV TEM were prepared from bulk alloy coupons by the back electropolishing method. An evaluation of electron optical techniques for the characterization of oxide films has been carried out previously.[15]

III. EXPERIMENTAL RESULTS

A. *Thermogravimetry*

The oxidation weight gain curves obtained at 400 and 480, and 520 and 575 °C under dry and wet 20 pct O_2/Ar are shown in Figures 1 and 2, respectively. With increasing temperature at the temperatures studied from 400 °C, the

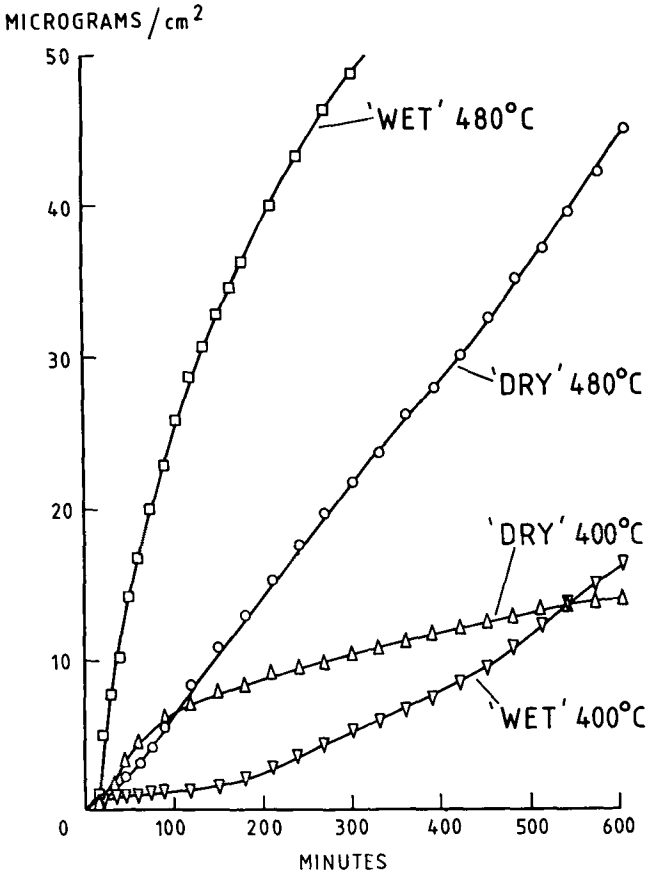

Fig. 1—Oxidation weight gain curves of Al-4.2 wt pct Mg reacted at 400 and 480 °C under dry and wet 20 pct O_2/Ar.

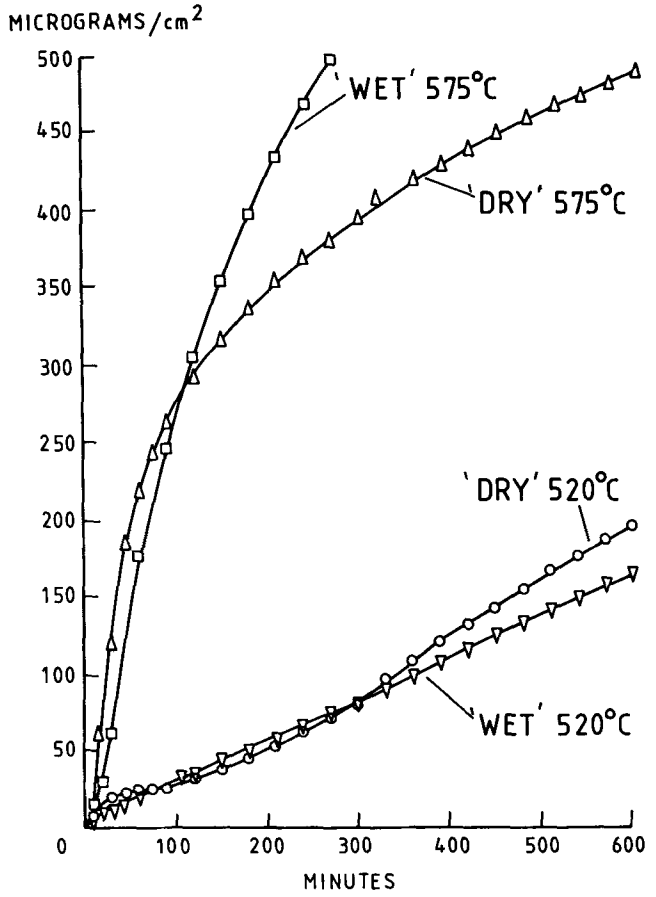

Fig. 2—Oxidation weight gain curves of Al-4.2 wt pct Mg reacted at 520 and 575 °C under dry and wet 20 pct O_2/Ar.

oxidation kinetics vary considerably, from logarithmic to para-linear, and finally to pseudo-parabolic type at 575 °C. The transition between pseudo-parabolic to linear kinetics observed in the para-linear weight gain curve obtained at 520 °C occurs between 100 and 210 minutes. It can be seen that water vapor modifies the weight gain curves obtained under the dry control condition, providing a reduction in weight gain during the early stages of oxidation at each of the temperatures studied except at 480 °C. In the later stages of oxidation, water vapor additions give higher weight gains except at 520 °C. At 400 °C under wet conditions, three linear portions to the weight gain curve can be discerned with breaks in slope at 150 and 400 minutes. Water vapor provides an inhibiting effect at this temperature up to about 550 minutes.

The kinetics were analyzed at 480 °C and found to conform to a power law with an exponent of 0.91. During the later stages of oxidation, the weight gains are significantly higher in the presence of water vapor. At 520 °C, the weight gains are approximately linear under the wet environment; however, in contrast to the other temperatures studied, water vapor results in a reduced overall weight gain in the later stages of oxidation. For this particular temperature, lower weight gains are also evident for the first 80 minutes of reaction, after which the weight gains become similar, until after 300 minutes there is a net beneficial effect. Water vapor provides a significant degree of oxidation inhibition in the early stages of oxidation at 575 °C, and the cross-over point occurs at 110 minutes; beyond this the weight gains are greater. The oxidation kinetics under the wet environment at 575 °C can be described as para-linear and were found to conform to a power law relationship with an exponent of 1.15.

B. *Microscopy—Dry Environments*

TEM of thin oxide films developed at 400, 480, and 520 °C (Figures 3, 4, and 5, respectively) showed that the oxide microstructure was morphologically duplex in nature; this duplex structure is typified in Figures 3(a) through (c) which show the oxide film after 1 hour at 480 °C. Dark-field imaging, Figure 3(b), reveals both the larger (primary) and smaller (secondary) crystallites in high contrast. The BF view of exactly the same area (Figure 3(a)), although indicating regions of film porosity, does not reveal the duplex structure so clearly. Close examination of the selected area diffraction pattern, Figure 3(c), shows that superimposed on the continuous oxide rings from the smaller secondary crystallites are spots from the coarser primary crystallites, confirming the duplex nature of the film. The oxide consists entirely of MgO randomly oriented with respect to the underlying matrix. Figures 4 and 5 are bright-field images of the oxidation product formed under dry conditions at 400 °C and 520 °C, respectively. Both primary and secondary morphologies of MgO are again evident. By comparing the micrographs in Figures 3(a), 4, and 5, corresponding to oxidation for 60 minutes at 480 °C, 600 minutes at 400 °C and 15 minutes at 520 °C, it can be seen that the secondary

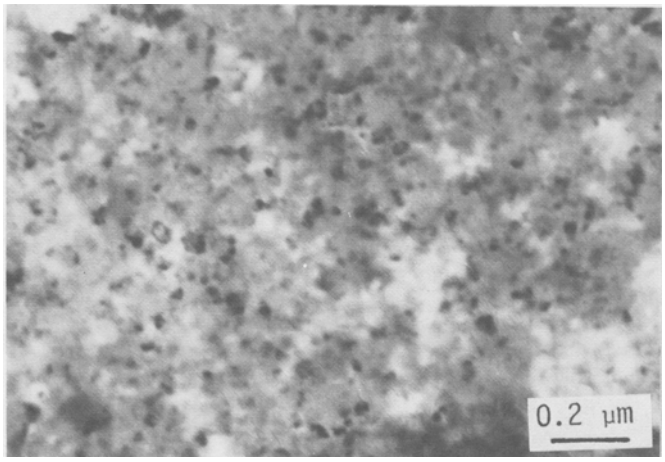

(*a*)

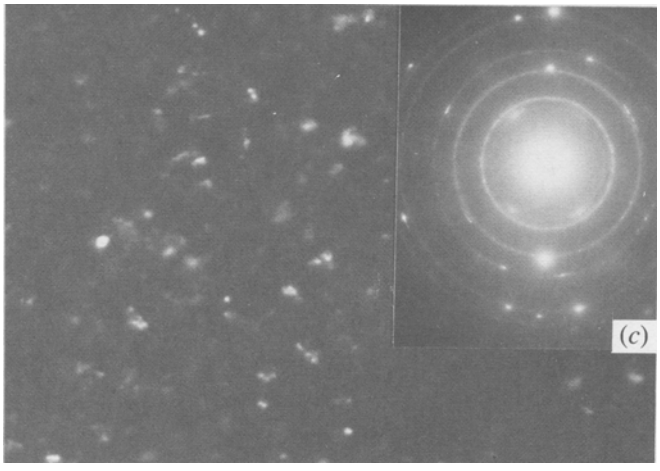

(*b*)

Fig. 3—(*a*) BF, (*b*) HROF, and (*c*) SADP electron micrographs of the same area of oxide film developed on Al-4.2 wt pct Mg oxidized for 60 min at 400 °C under dry 20 pct O_2/Ar.

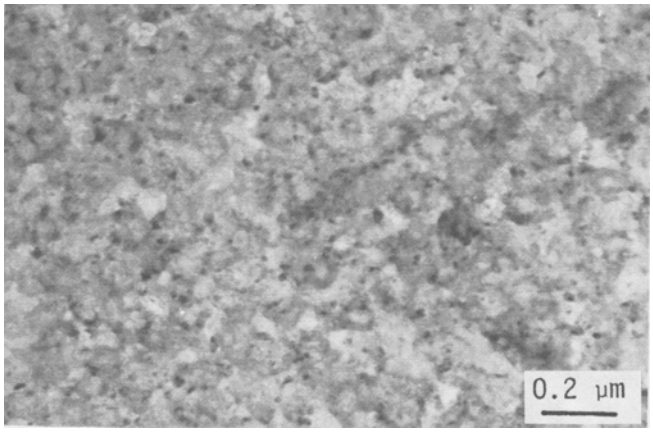

Fig. 4—Bright-field micrograph of the oxide film developed after 600 min reaction at 400 °C under dry 20 pct O_2/Ar.

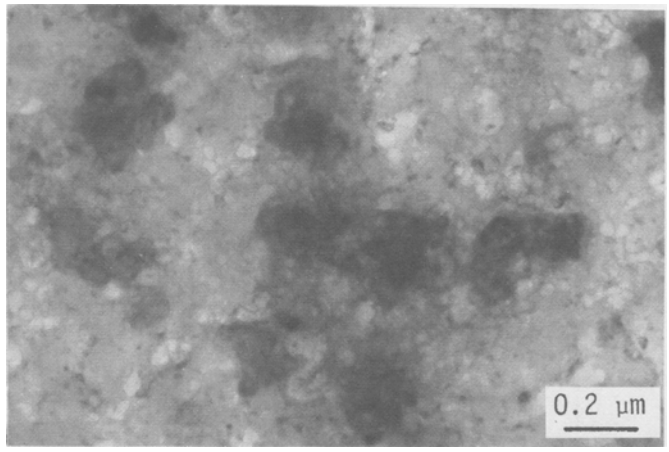

Fig. 5—Bright-field micrograph of the oxide following 15 min reaction at 520 °C under dry 20 pct O_2/Ar.

crystallites remain approximately constant in size (~50 Å), but that the primary MgO crystals decrease in size with temperature, from ~2000 Å at 520 °C, to ~1000 Å at 480 °C and ~500 Å at 400 °C.

Scanning electron microscopy of the films was undertaken to correlate oxide surface topography with position along the various weight gain curves. At points corresponding to regions where linear nonprotective kinetics of oxidation were produced, the films were found to be extremely porous, consisting of loosely packed agglomerates of primary crystals. By contrast in regions of decreasing reaction rates, the films were relatively smooth with isolated agglomerates of primary oxides penetrating the reduced γ-Al_2O_3 overlayer. An example of this is shown in Figure 6, which is an SEM stereo pair of the oxide film topography developed at 520 °C for 5 minutes under dry conditions.

Stereo pairs showing the development of the porous films after exposures of 40, 100, and 200 minutes, corresponding to the pseudo-parabolic, transitional, and linear regions of the weight gain curves at 520 °C, are presented in Figure 7. The stereo-view (Figure 7(a)) of the oxide film topography corresponding to the pseudo-parabolic branch of oxidation shows a relatively smooth surface. Further oxidation to the transition point (100 minutes), Figure 7(b), results in an irregular oxide/oxygen interface. Stereo-viewing reveals that towers of primary MgO crystals (characteristic of the linear regimes of oxidation) are developing at a large number of growth sites. Extended oxidation to the linear regime results in fewer reaction sites and coarse agglomerations of primary MgO (Figure 7(c)).

C. *Microscopy—Wet Conditions*

TEM (Figures 8(a) and (b)) of the film developed at 480 °C after 60 minutes under 20 °C w.v.s. 20 pct O_2/Ar show that the surface film morphology and crystallography are similar to that observed under dry conditions, but, qualitatively, there is an increased density of primary crystallites under comparable wet oxidizing conditions. Furthermore, stereo-imaging of the oxide topography (Figure 9(d)) revealed that the addition of water vapor to the oxidizing atmosphere promotes a flatter, more even oxide topography, and the amorphous overlayer is preserved for longer periods. A visual comparison of specimens oxidized for

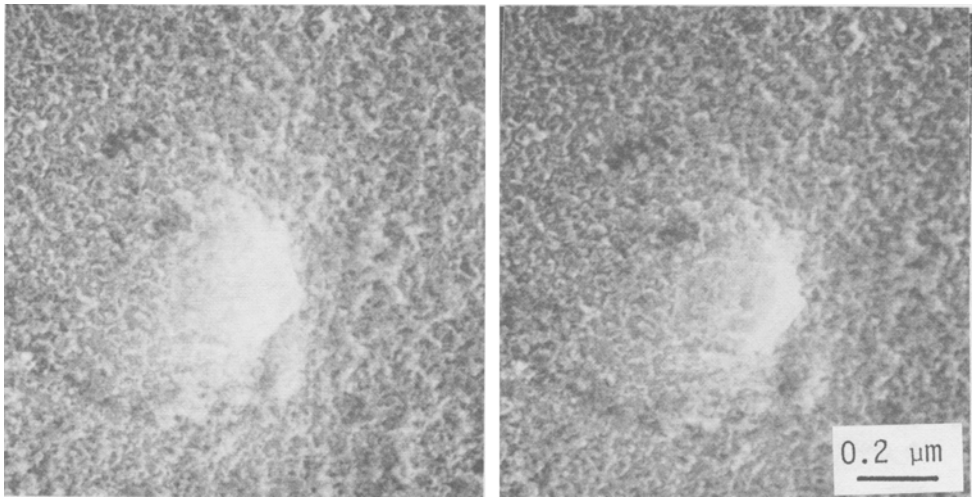

Fig. 6—Stereo SEM image of Al-4.2 wt pct Mg oxidized at 520 °C for 5 min under dry 20 pct O_2/Ar showing penetration of the amorphous γ-Al_2O_3 overlayer by a group of primary oxides.

extended periods (~600 minutes) under both wet and dry conditions showed that water vapor promotes a shiny grey/black surface film in contrast to the matt black films characteristic of the dry environment.

IV. DISCUSSION

Under dry oxidizing conditions, the reaction kinetics for this alloy are strongly temperature dependent, progressing from logarithmic to linear, para-linear, and pseudo-parabolic with increasing temperature from 400 °C to 575 °C (Figures 1 and 2). Para-linear oxidation kinetics have been reported previously for Al-4.6 wt pct Mg[11] and Al-3 wt pct Mg[2] alloys at about 500 °C, and in addition the S-shaped branch of the weight gain curve at 400 °C (Figure 1) is consistent with the study of Grauer and Schmoker.[11] Other than at the above temperatures the oxidation kinetics for this alloy are at variance with those observed in previous studies. It is considered that these differences arise out of differences in surface preparation prior to oxidation, which are known to have a dominant effect on surface reactivity.[3]

Under wet oxidizing conditions and in the early stages of oxidation, water vapor additions were found to be beneficial over the temperature range studied except at 480 °C. In contrast with the other temperatures studied, at 520 °C reduced oxidation weight gains were observed during the later stages of exposure to the water containing environment. For this environment the oxidation kinetics can be described as asymptotic, pseudo-parabolic, linear, and pseudo-parabolic at 400, 480, 520, and 575 °C, respectively. Previous studies have reported both beneficial[12,16] and detrimental[3] effects of water vapor on the oxidation of Al-Mg alloys. It would thus appear from these studies that surfaces on Al-Mg alloys prepared by electropolishing have a reduced reactivity in water containing oxidizing atmospheres compared to surfaces prepared by chemical or electrochemical processes.

TEM examination of oxide films developed on these alloys shows that during the early stages of their growth the surface films are duplex, consisting of both the residual amorphous overlayer decomposed by magnesium and microcrystalline magnesium oxides. Oxide films produced during extended oxidation consist exclusively of coarse agglomerations of microcrystalline MgO. In this situation no one oxidation theory is applicable and the fitting of mathematical functions to the weight gain data (*e.g.*, Reference 2) loses its significance other than providing a convenient method of expressing the data.

Two distinct modes of crystalline oxide formation on Al-Mg alloys have been identified[7,10,15] which have been termed[7] primary and secondary, respectively. These are defined as follows:

Primary: An oxide phase formed by the direct reaction of a metal and oxygen.

Secondary: An oxide phase formed by the reduction, reaction, crystallization, or the decomposition of an existing oxide film.

In this study the crystalline oxides have been identified as exclusively MgO, the primary oxides located at the oxide metal interface and secondary oxides contained within the amorphous overlayer resulting from the secondary reduction reaction with magnesium[7,11] (Eq. [1]). Primary magnesium oxides form on Al-Mg alloys in a manner analogous to the nucleation and growth of primary, crystalline γ-Al_2O_3 on pure aluminum.[7] The absence of an induction period[7] and appearance at much lower temperatures of crystalline oxides on Al-Mg alloys[17] (350 °C compared to 475 °C for pure aluminum) is due to enhanced oxygen ion transport through the amorphous overlayer as a result of doping by divalent magnesium ions from the alloy substrate. In terms of oxide nucleation and growth, primary MgO formation differs from crystalline γ-Al_2O_3 in that MgO penetrates both the alloy substrate and the amorphous overlayer. The oxidation weight gain curves shown in Figures 1 and 2 can be described in terms of a model based on disruption of a protective overlayer by penetrating magnesium oxides which vary in size with temperature.

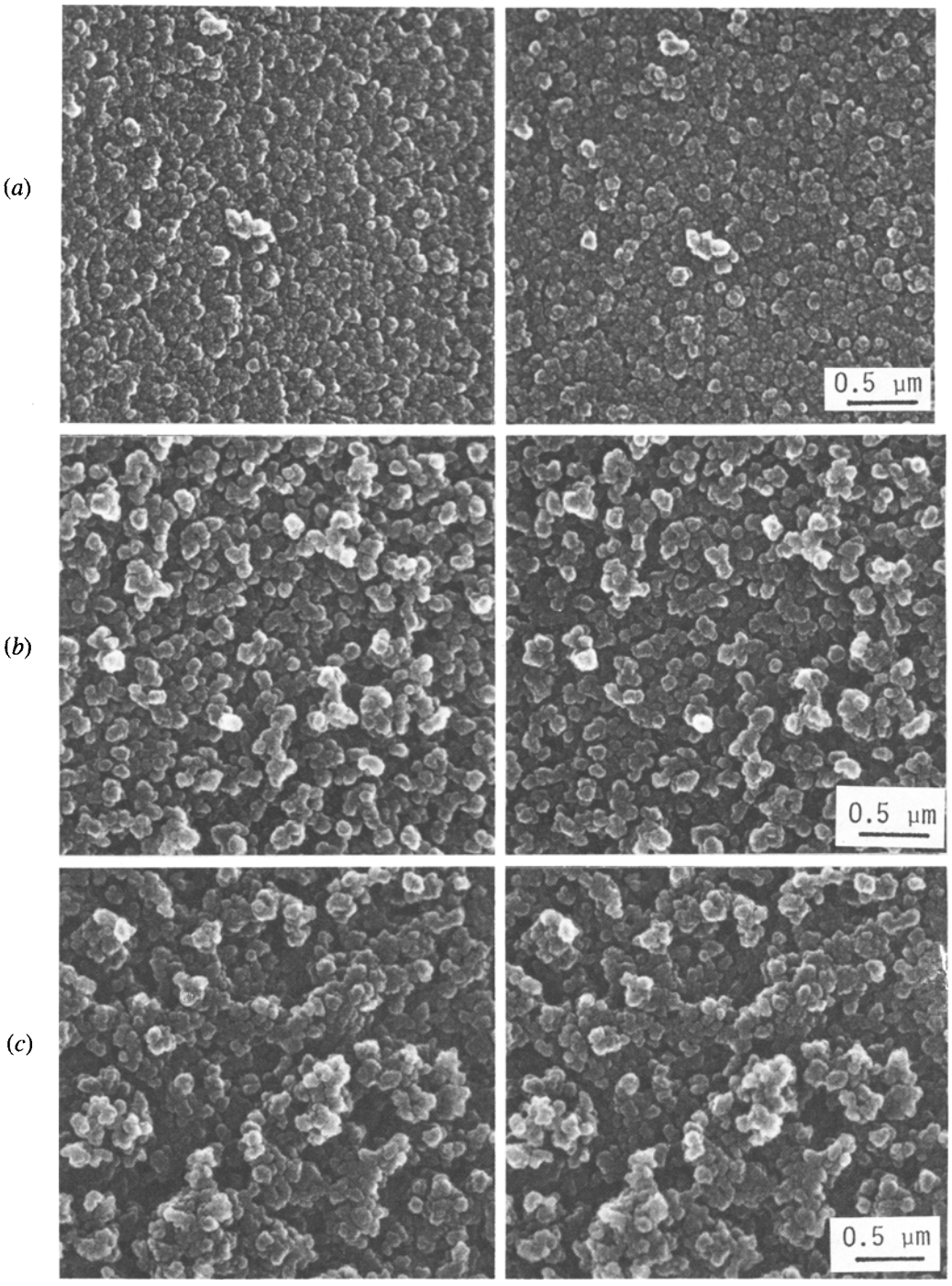

Fig. 7—Stereo SEM images of the oxide topography on Al-4.2 wt pct Mg reacted at 520 °C under dry 20 pct O_2/Ar for periods of (*a*) 40 (20 deg tilt), (*b*) 100 (15 deg tilt), and (*c*) 200 min (10 deg tilt) corresponding to the observed pseudo-parabolic transitional and linear regimes of oxidation at this temperature.

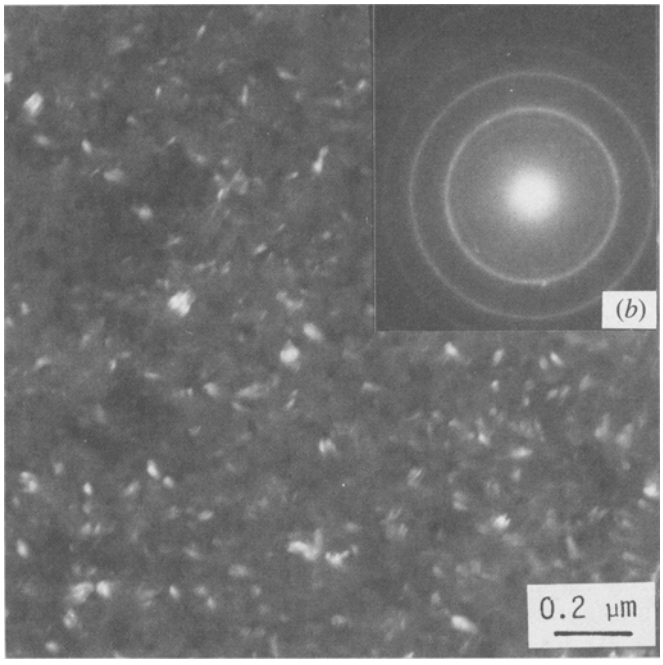

(*a*)

Fig. 8—(*a*) HRDF and (*b*) SAD images of the oxide film developed after 60 min reaction at 480 °C under wet 20 pct O_2/Ar.

Oxidation Model for Al-4.2 Wt Pct Mg

During the initial stages of oxidation at temperatures in excess of 350 °C, the transport of oxygen to the amorphous oxide/metal interface is rapid and an oxygen saturated layer develops in the surface layers of the alloy substrate, as shown schematically in Figure 10. Provided the amorphous film remains relatively intact, oxidation will be controlled by diffusion of oxygen through the film. The oxidation kinetics at this stage would be expected to be either logarithmic or parabolic; presumably this has escaped detection by being within the timescale of beginning the weight gain measurements of this work.

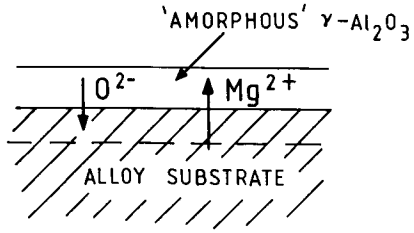

Fig. 10—Schematic diagram of the initial stages of Al-4.2 wt pct Mg oxidation, showing doping of amorphous γ-Al_2O_3 overlayer by Mg^{2+} and oxygen transport to the oxide metal interface.

Nucleation and growth of primary MgO occurs once the critical oxygen concentration in the alloy substrate has been exceeded. The experimental observations show that the primary oxide size increases with temperature from approximately 500 Å at 400 °C to 2000 Å at 520 °C. These observations may be explained in terms of the increasing diffusivity of oxygen with temperature in the alloy substrate giving rise to a greater depth of oxygen saturation and hence 'primary' oxide size. HRSEM of the oxide surface topography after the nucleation and growth of primary MgO at 520 °C (Figure 6(a)) shows that these oxides grow toward the oxide/oxygen interface. If it is assumed that the height of oxide penetration into the amorphous film is proportional to the primary oxide diameter, then two situations may be envisaged where (1) the primary oxide penetration is insufficient to disrupt the amorphous overlayer, which remains relatively intact, *i.e.*, at low temperatures; (2) primary oxide penetration causes cracking of the amorphous overlayer and therefore rapid short circuit diffusion of oxygen to the oxide/metal interface, *i.e.*, at high temperatures. This is shown schematically in Figure 11.

Cracking of the amorphous film by primary penetration will lead to a rapid ingress of oxygen and faster oxidation kinetics. This event represented by Figure 12 can be considered as the microstructural feature which changes the oxidation kinetics from parabolic, *e.g.*, Figure 11, to linear *e.g.*, Figures 13 and 14. It is proposed that surfaces which come into contact with the environment after being defilmed

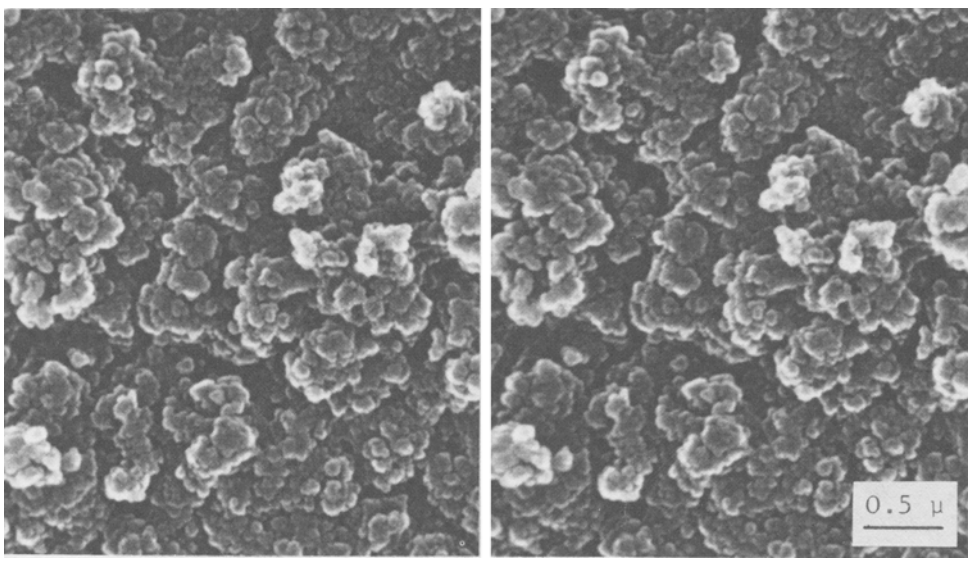

Fig. 9—Stereo SEM image of the surface topography on Al-4.2 wt pct Mg reacted under wet 20 pct O_2/Ar at 520 °C for 200 min.

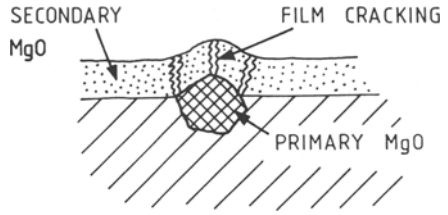

Fig. 11 — Schematic showing disruption of the amorphous overlayer by primary oxide nucleation and growth. At this stage secondary oxides of MgO become apparent.

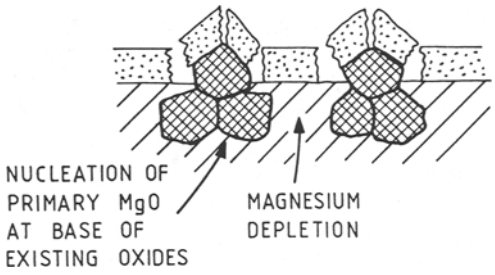

Fig. 12 — Oxidation proceeds by the repeated nucleation and growth of primary MgO oxides at the bases of preexisting primaries. Magnesium depletion occurs between the stacks of oxides.

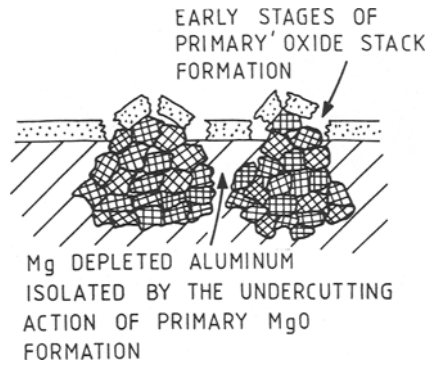

Fig. 13 — With further oxidation primary oxide formation and penetration continues. Sections of the alloy substrate are undercut. This figure is on a coarser scale than Figs. 10 through 12.

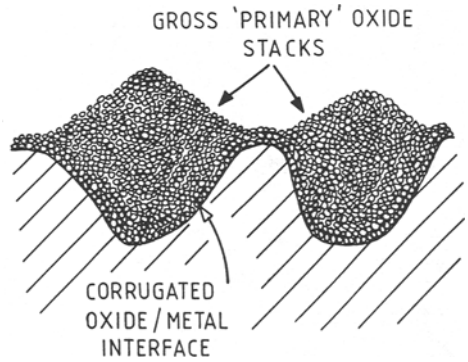

Fig. 14 — Following extended oxidation particularly at high temperatures, thick oxide films and a highly corrugated oxide/metal interface develop. This figure is on an even coarser scale than the preceding figure.

by primary growth immediately develop a fresh overlayer of Mg^{2+} doped γ-Al_2O_3 beneath which further primary nucleation and growth takes place. At this stage of the oxidation process, secondary MgO may be discerned. The effect of secondary reduction on the amorphous film's mechanical and physical properties is not understood; however, it is likely that this reaction will be detrimental, causing the film to become weaker.

Thicker films result from the repeated nucleation and growth of primary MgO at the base of existing primary crystallites to form stacks of primary oxides. An example of nucleation at the base of an existing primary oxide is shown in Figure 5(a) (at 520 °C) and represented schematically in Figure 12.

In this situation the regions of metal between the primary oxide stacks will be denuded in magnesium, and will be relatively inert. Oxidation is localized therefore at the sites of existing primary oxides. If the nucleation rate of the primary oxides was constant, then linear oxidation kinetics would be expected, such as observed at 480 °C (Figure 1). This stage (represented in Figure 13) is the initiation of the massive stacks of primary oxides observed at 520 °C after 200 minutes oxidation (Figure 7(c)).

Oxidation continues by the further nucleation and growth of primary oxides at the base of existing oxides. Primary oxide nucleation and growth is favored at these sites because magnesium is readily supplied from the bulk alloy and can combine with oxygen supplied *via* short circuit diffusion paths down the primary oxide/metal boundaries. A corrugated oxide/metal interface develops as a result of this mode of oxidation. This situation is shown schematically in Figure 14.

Any region of the alloy substrate which is undercut by primary oxide penetration will become completely denuded in magnesium and remain incorporated in the oxide film. This would account for the detection using X-ray diffraction of elemental aluminum in surface films of MgO grown on Al/Mg alloys.[2,4] At higher temperatures where the primary oxides are coarser (*i.e.*, 520 °C), the oxide metal interface becomes correspondingly coarser with an acceleration in the oxidation rate (shown schematically in Figure 14).

Indirect evidence for the development of a corrugated oxide/metal interface is shown in the sequence of stereo pairs Figures 7(a) through (c) which show the oxide topography after 40, 100, and 200 minutes, corresponding to the pseudo-parabolic, transitional, and linear regimes of paralinear oxidation at this temperature. These observations provide further evidence for the validity of oxidation mechanism shown schematically in Figures 10 through 14.

Using the above model, the effect of water vapor can be rationalized in providing a general inhibiting effect during the first stages of oxidation. We take as a starting point the mechanical test data of Grosskreutz[18] showing the dependence of Young's modulus, fracture stress, and fracture strain of thin anodic films on the water vapor content of the test atmosphere. The results are shown in Table I. The geometric effects on oxide film fracture during oxidation have been analyzed by Manning.[19,20]

Table I. Mechanical Properties (Room Temperature) of 300 nm Thick Amorphous Anodic γ-Al_2O_3 Films Tested at Atmospheric Pressure and 1.33×10^{-4} Pa (Grosskreutz[18])

Test Atmosphere, Pa	Young's Modulus, Pa	Fracture Stress, Pa	Fracture Strain
1.013×10^5 (lab air)	$5.47 \pm 2.72 \times 10^{10}$	1.75×10^8	3.54×10^{-3}
1.33×10^{-4}	$2.13 \pm 0.69 \times 10^{11}$	2.52×10^8	1.52×10^{-3}

The critical thickness of a growing oxide film which can accommodate a given radius of curvature without cracking is given by:[19]

$$h_{crit} = \left| 12 \frac{\gamma}{E} \frac{R^2}{M^2 \phi} \right|^{1/3} \quad [2]$$

where h_{crit} = critical thickness of oxide film,
γ = surface energy of oxide fracture surface,
E = Young's modulus,
R = radius of interface curvature,
M = scale displacement vector, and
ϕ = Pilling-Bedworth ratio

This equation has been applied by Manning to the cracking of hard anodized coatings on aluminum,[20] where it was shown that the values calculated using this expression compared closely with literature values of critical bending radii.

Using this equation and the data of Table I, in conjunction with the model developed for Al-Mg oxidation, we calculate the critical amorphous oxide film overlayer thicknesses to withstand primary oxide penetration without cracking. This is particularly applicable to the situation depicted in Figure 11. Typical values for ϕ and M for hard anodized films on aluminum have been given as 2.1 and 0.287, respectively.[20] The results are presented in Table II and were calculated assuming $\gamma = 2$ J/m^2 and using the data for anodic films tested under wet, *i.e.*, lab air at atmospheric pressure and dry, *i.e.*, vacuum (Table I) conditions. They show that γ-Al_2O_3 films have a substantially greater resistance to cracking in the presence of water vapor than without. According to Reference 6, at high temperatures the oxide film on aluminum grows to about 17.6 nm thickness at 500 °C and 5.4 nm at 450 °C. These values are of the same order as the critical thicknesses shown in Table II, lending credence to the calculations. It is therefore feasible that the beneficial effect of water vapor in reducing the oxidation weight gains at 400 °C, and in the early stages at 520 and 575 °C (Figures 1 and 2), is due to water vapor inhibiting oxide film fracture.

The consistently higher weight gains at 480 °C due to water vapor (Figure 1) do not conform with this general scheme for reasons which are not yet understood. At present no information is available regarding the mechanical properties of thin amorphous films at high temperatures under moist atmospheres. A discontinuous change in properties or film structure may account for the enhanced weight gains observed at 480 °C. Although the formation of hydrous films at high temperatures is a possibility, within the resolution of electron diffraction, no hydrous species were detected after 60 minutes oxidation at 480 °C (Figure 8(b)) under wet 20 pct O_2/Ar. Enhanced weight gains due to water vapor may be expected in the later stages of oxidation due to hydrogen damage generating new and increased areas of metal surface for subsequent reaction.[12]

Table II. Calculated Amorphous γ-Al_2O_3 Critical Oxide Thicknesses for Fracture Due to Primary Oxide Penetration, Using Analysis of Manning[20] and Data of Grosskreutz[18]

Test Environment (Grosskreutz[18]), Pa	Primary Oxide Radius, nm	h_{crit} nm
1.013×10^5 wet	100 (520 °C)	29.4
	50 (480 °C)	19.3
	25 (400 °C)	11.6
1.33×10^{-4} dry	100 (520 °C)	18.9
	50 (480 °C)	12.2
	25 (480 °C)	7.5

V. CONCLUSIONS

The high temperature oxide films which develop on Al-4.2 wt pct Mg are essentially microcrystalline MgO and consist of two types of MgO, termed primary and secondary oxides, dependent on the mechanism of formation. Primary oxidation is the direct reaction between magnesium from the alloy substrate with oxygen to form MgO which occurs at the oxide/metal interface. Secondary oxidation is the solid state reduction of the original air formed film of amorphous γ-Al_2O_3 by Mg from the alloy substrate to form MgO. The oxidation weight gain curves can be explained in terms of a microstructural model based on disruption of a protective amorphous overlayer by penetrative primary MgO and subsequent development of a corrugated oxide/metal interface. The beneficial effect of water vapor in reducing oxygen uptake in the first stages of oxidation may be rationalized in terms of water vapor improving the resistance of the protective amorphous film to rupture. Critical oxide film thickness values have been calculated using the analysis developed by Manning[19] for film cracking.

ACKNOWLEDGMENTS

The authors would like to thank Alcan International Limited, Banbury Laboratories and the Science and Engineering Research Council for financial support.

REFERENCES

1. M. Whitaker and A.R. Heath: *J. Inst. Metals*, 1953-54, vol. 82, pp. 107-16.
2. W.W. Smeltzer: *J. Electrochem. Soc.*, 1958, vol. 105, no. 2, pp. 67-71.
3. C.N. Cochran and W.C. Sleppy: *J. Electrochem. Soc.*, 1961, vol. 108, no. 4, pp. 322-27.
4. P.E. Blackburn and E.A. Gulbransen: *J. Electrochem. Soc.*, 1960, vol. 107, no. 12, pp. 944-50.
5. P.E. Doherty and R.S. Davis: *J. App. Phys.*, 1963, vol. 34, no. 3, pp. 619-28.

6. A. F. Beck, M. A. Heine, E. J. Caule, and M. J. Pryor: *Corros. Sci.*, 1967, vol. 7, pp. 1-22.
7. G. M. Scamans and E. P. Butler: *Metall. Trans. A*, 1975, vol. 6A, pp. 2055-63.
8. G. M. Scamans and E. P. Butler: *Proc. Quatrieme Congres International Microscopie Electronique Haute Tension*, Toulouse, 1975, pp. 341-44.
9. A. J. Brock and M. J. Pryor: *Corros. Sci.*, 1973, vol. 13, pp. 199-227.
10. A. J. Brock and M. A. Heine: *J. Electrochem. Soc.*, 1972, vol. 119, no. 8, pp. 1124-27.
11. R. Grauer and P. Schmoker: *Werkstoffe und Korrosion*, 1976, vol. 27, pp. 769-74.
12. R. A. Hine and R. D. Guminski: *J. Inst. Metals*, 1960-61, vol. 89, pp. 417-22.
13. I. M. Ritchie, J. V. Sanders, and P. L. Weickhardt: *Oxidation of Metals*, 1971, vol. 3, no. 1, pp. 91-101.
14. G. M. Scamans and A. S. Rehal: *J. Mat. Sci.*, 1979, vol. 14, pp. 2459-70.
15. D. J. Field, E. P. Butler, and G. M. Scamans: *Inst. Phys. Conf. Ser. No. 52*, 1980, pp. 401-04.
16. C. Lea and J. Ball: *Applications Surf. Sci.*, 1984, vol. 17, pp. 344-62.
17. L. de Brouckere: *J. Inst, Metals*, 1945, vol. 71, pp. 131-47.
18. J. C. Grosskreutz: *Surf. Sci.*, 1967, vol. 8, pp. 173-90.
19. M. I. Manning: *Proc. Ausbul von Oxidshichtem auf Hochtemperatur Werkstoffen und Erihre Techniche Bechutang*, Ausburg, pub. DGM, A. Rahmel, ed., 1983, pp. 283-97.
20. M. I. Manning: *Corros. Sci.*, 1981, vol. 21, (4), pp. 301-16.